Autonomic Neuroscience: Basic and Clinical 136 (2007) 43–51

AUTONOMIC NEUROSCIENCE: Basic & Clinical

www.elsevier.com/locate/autneu

Sympathetic nerve activity and heart rate variability during severe hemorrhagic shock in sheep ☆

Andriy I. Batchinsky [a,*], William H. Cooke [b], Tom A. Kuusela [c], Bryan S. Jordan [a], Jing Jing Wang [a], Leopoldo C. Cancio [a]

[a] U.S. Army Institute of Surgical Research, 3400 Rawley E. Chambers Avenue, Building 3611, Fort Sam Houston, Texas, 78234-6315, United States
[b] Laboratory for Applied Autonomic Neurophysiology, Department of Health and Kinesiology, University of Texas, San Antonio, 6900 North Loop 1604 West San Antonio, Texas, 78249, United States
[c] Department of Physics, University of Turku, Turku, Finland

Received 30 January 2007; received in revised form 28 March 2007; accepted 30 March 2007

Abstract

Introduction: In this study we explored direct and indirect measures of autonomic nervous system function, as well as changes in cardiovascular complexity, during hemorrhagic shock (HS).
Methods: HS was induced in anesthetized sheep ($n=8$) by removing 40 ml/kg of blood in four 10 ml/kg steps over 40 min. Resuscitation was performed with lactated Ringer's and re-infusion of shed blood. Renal sympathetic nerve activity (RSNA) was measured by microneurography. Spectral analysis of heart rate variability (HRV) employed fast-Fourier transformation of the R-to-R interval (RRI) of the EKG. This generated the normalized high-frequency (HFnu) and low-frequency (LFnu) powers of the RRI, and their ratio (LFnu/HFnu, a proposed index of sympatho-vagal balance). Additionally, non-linear methods were applied: RRI complexity was measured by approximate (ApEn) and sample (SampEn) entropy methods; RRI fractal dimension was measured by curve lengths (FDCL). Plasma catecholamines were determined by HPLC.
Results: The model caused profound HS; 2/8 animals survived till the end of resuscitation. RSNA increased in 7/8 sheep and, as HS progressed, multiple burst complexes were identified followed by sympathetic withdrawal. Concomitant decreases in HFnu and increases in LFnu/HFnu occurred after 20 ml/kg blood loss. ApEn and FDCL decreased after withdrawal of 40 ml/kg of blood. Catecholamine concentrations increased throughout HS. LFnu/HFnu and RSNA were not linearly correlated.
Conclusions: HS led to an increase in RSNA with subsequent withdrawal. LFnu/HFnu increased during HS in association with vagal withdrawal and loss of RRI complexity. RRI complexity may in part reflect vagal modulation of the heart rate. Changes in directly measured tonic sympathetic traffic do not correlate with non-invasive measures of autonomic modulation of the heart.

Keywords: Autonomic nervous system; Renal sympathetic nerve activity; Hemorrhagic shock; Heart rate variability; Spectrum analysis; Non-linear analysis; Complexity; Entropy

1. Introduction

The autonomic response to hemorrhagic shock (HS) is complex, under-investigated and influenced by the dynamics and magnitude of volume depletion (Secher et al., 1992; Evans et al., 2001). Animal studies involving direct renal neural recordings during HS showed increased renal sympathetic nerve activity (RSNA) as the initial response to volume loss (Skoog et al., 1985; Koyama et al., 1988, 1992; Malpas et al., 1998). With progression of shock, a decrease in RSNA may

Abbreviations: HS, Hemorrhagic shock; HF, high-frequency power; LF, low-frequency power; RSNA, renal sympathetic nerve activity; RRI, R-to-R interval of the EKG; LR, lactated Ringer's; ApEn, approximate entropy; SampEn, sample entropy; FDCL, fractal dimension by curve lengths.

☆ The opinions or assertions contained herein are the private views of the authors and are not to be construed as official or as reflecting the views of the Department of the Army or the Department of Defense.

* Corresponding author.
E-mail address: andriy.batchinsky@amed.army.mil (A.I. Batchinsky).

1566-0702/$ - see front matter © 2007 Elsevier B.V. All rights reserved.
doi:10.1016/j.autneu.2007.03.004

Report Documentation Page

Form Approved
OMB No. 0704-0188

1. REPORT DATE	2. REPORT TYPE	3. DATES COVERED
30 OCT 2007	**N/A**	**-**

4. TITLE AND SUBTITLE	5a. CONTRACT NUMBER
Sympathetic nerve activity and heart rate variability during severe hemorrhagic shock in sheep	5b. GRANT NUMBER
	5c. PROGRAM ELEMENT NUMBER
6. AUTHOR(S)	5d. PROJECT NUMBER
Batchinsky A. I., Cooke W. H., Kuusela T. A., Jordan B. S., Wang J. J., Cancio L. C.,	5e. TASK NUMBER
	5f. WORK UNIT NUMBER
7. PERFORMING ORGANIZATION NAME(S) AND ADDRESS(ES)	8. PERFORMING ORGANIZATION REPORT NUMBER
United States Army Institute of Surgical Research, JBSA Fort Sam Houston, TX 78234	
9. SPONSORING/MONITORING AGENCY NAME(S) AND ADDRESS(ES)	10. SPONSOR/MONITOR'S ACRONYM(S)
	11. SPONSOR/MONITOR'S REPORT NUMBER(S)

12. DISTRIBUTION/AVAILABILITY STATEMENT
Approved for public release, distribution unlimited

13. SUPPLEMENTARY NOTES

14. ABSTRACT

15. SUBJECT TERMS

16. SECURITY CLASSIFICATION OF:			17. LIMITATION OF ABSTRACT	18. NUMBER OF PAGES	19a. NAME OF RESPONSIBLE PERSON
a. REPORT	b. ABSTRACT	c. THIS PAGE			
unclassified	**unclassified**	**unclassified**	**UU**	**9**	

occur (Skoog et al., 1985; Koyama et al., 1988, 1992) as a sign of irreversible shock (Koyama et al., 1988).

Because direct tonic nerve activity measurements are invasive, they are not usable as clinical monitoring tools. Alternatively, analysis of the R-to-R-interval (RRI) by fast-Fourier transform has been proposed as an indirect index of cardiac autonomic modulation (Akselrod et al., 1981; Pagani et al., 1986). The low-frequency component of the RRI power spectrum, or low-frequency (LF) power, is influenced by both sympathetic and parasympathetic activity. High-frequency power (HF), by contrast, is influenced by parasympathetic activity alone. The ratio of LF to HF (LF/HF) has been proposed as an index of "sympatho-vagal balance" (Pagani et al., 1986). The concept of sympatho-vagal balance, however, has been critically appraised (Parati et al., 1995; Eckberg, 1997; Notarius and Floras, 2001). At present, the indirect heart rate variability (HRV) metrics are said to reflect cardiac autonomic influences in a qualitative manner, and their full meaning remains controversial (Parati et al., 2006).

Despite this controversy, HRV metrics are widely used for obtaining indirect non-invasive insight into cardiovascular autonomic modulation (Anonymous, 1996). Association of HRV metrics with volume status (Butler et al., 1994; Palazzolo et al., 1998; Goldstein et al., 1999; Batchinsky et al., 2007) and with mortality in ICU (Winchell and Hoyt, 1996) and trauma patients (Cooke et al., 2006) has suggested their potential utility as clinical monitoring tools (Winchell and Hoyt, 1996; Grossman et al., 2004; Cooke et al., 2006; Parati et al., 2006).

Saul et al. (1990) reported a positive correlation between the LF/HF ratio and directly measured sympathetic nerve activity in humans, while others have not (Kingwell et al., 1994; Pagani et al., 1997; Cooke et al., 1999; Cooke and Dowlyn, 2000). Kingwell et al. (1994) reported dissociation between the LF and cardiac sympathetic activity evaluated by norepinephrine spillover. In animal studies that did not involve direct RSNA recordings, RRI LF increased during hemorrhage in conscious dogs (Madwed and Cohen, 1991), decreased during hypovolemic shock in anesthetized rabbits (Goldstein et al., 1999), and showed a differential response in tachycardic and bradycardic hemorrhaged dogs (Kawase et al., 2000).

In this study we sought to characterize the changes in RSNA and its morphology occurring in response to severe HS in sheep, and to determine the relationship, if any, between the indirectly assessed LF/HF ratio of the RRI and directly measured tonic RSNA. We hypothesized that HS would cause concurrent increases in both the LF/HF ratio and RSNA, possibly followed by withdrawal of RSNA in pre-terminal subjects. We also hypothesized that HS would be associated with loss of RRI complexity, a new metric derived from non-linear biosignal analysis methods, which quantifies RRI irregularity by assessment of structural changes within the signal (Pincus, 1995; Porta et al., 1998; Richman and Moorman, 2000).

2. Materials and methods

This study was approved by the U.S. Army Institute of Surgical Research Animal Care and Use Committee and was carried out in accordance with the guidelines set forth by the Animal Welfare Act and other federal statutes and regulations relating to animals and studies involving animals and by the 1996 Guide for the Care and Use of Laboratory Animals of the National Research Council.

2.1. Animal preparation

Neutered male sheep ($n=8$), weighing 35.9±1.9 kg were fasted for 24 h prior to the study, premedicated by ketamine, induced with isoflurane via mask and endotracheally intubated. With the animal in dorsal recumbency, surgical anesthesia was carried out with a combination of isoflurane (0.47±0.03%) and intravenous ketamine (468±3.7 μg/kg/h) (KetaVed, Ketamine HCL, Phoenix, Scientific, Inc., St. Joseph, MO). Animals were ventilated in volume-control mode with a tidal volume of 13 ml/kg, respiratory rate of 12 per min and fraction of inspired oxygen of 100%. Tidal volume and respiratory rate were adjusted to maintain the end tidal level of CO_2 between 30 and 40 mm Hg. Bilateral surgical catheterizations of the right external jugular vein and both femoral arteries and veins were performed followed by a midline laparotomy and splenectomy to exclude the possibility of splenic auto-resuscitation during hemorrhage. Each animal then received a 1-l bolus of lactated Ringer's (LR) solution followed by a maintenance infusion of LR at 2 ml/kg/h. Next, the left kidney was exposed, the renal nerve dissected and a unipolar Tungsten metal microelectrode with a 75-μm shaft (FHC, Bowdoinham, ME) inserted into the nerve. After the bursts were visually verified the electrode was glued in place with cyanoacrylate adhesive (Vetbond, 3M, Saint Paul, MN).

2.2. Physiologic measurements

Arterial plasma lactate was measured with an i-STAT blood gas analyzer (Abbot Laboratories, East Windsor, NJ). Standard four-lead EKG was obtained from surface electrodes glued to the previously depilated skin in the axillae and outer thighs. A continuous cardiac output pulmonary arterial catheter (Model 746HF8, Edwards Lifesciences LLC, Irvine, CA) was placed via the left external jugular vein. Arterial pressure was transduced (Transpac® IV, Abbott, North Chicago, IL) at heart level. All physiologic waveforms were displayed continuously using a clinical monitor (Viridia CMS 2000, Boebingen, Germany).

2.3. Experimental protocol

After a steady nerve signal was obtained (verified visually and by auscultation) the experimental protocol was started. Animals were bled in four 10-min cycles, each followed by a

15-min observation period. Blood was manually withdrawn via a syringe from the femoral arterial line during each 10-min bleeding period at a constant rate of 1 ml/kg/min for a total bleed volume (all four cycles) of 40 ml/kg. The removed blood was collected into commercial blood-collection bags containing CPD anticoagulant (Terumo Corp., Tokyo, Japan). After the fourth hemorrhage segment and observation period, sheep were resuscitated with 3 times the shed blood volume with LR over a period of 25 min, were observed for 15 min, and were given their shed blood back via infusion over 25 min. Resuscitation was accomplished with the Model 245 Ranger (Blood/Fluid) Warming system (Augustine Medical Inc, Eden Prairie, MN). Following a final 15-min period after re-infusion, surviving animals were euthanized by means of an overdose of sodium pentobarbital (Fatal-Plus, Dearborn, MI).

2.4. Nerve signal analysis

RSNA signals were amplified (90,000 times) and filtered at low- and high-frequency cut-offs of 0.7 and 2 kHz respectively using a Nerve Traffic Analysis System (Model 662C-4; University of Iowa Bioengineering, Iowa City, IA). The presence of bursts was verified both visually and by auscultation. Automatic amplitude-based detection of sympathetic bursts was performed with WinCPRS software (Absolute Aliens Oy, Turku, Finland). Off-line, the signal in all files was brought to a common baseline via global polynomial fitting with the order of 4 and the trends were removed using the Butterforth high pass filter with the cut-off frequency of 0.005. RSNA was calculated with an averaging window width of 5 s and average window step of 1 s using mean normalization. Discrete RSNA data files were selected during the observation periods, and were normalized with the baseline activity as the reference value. A scaling factor was applied, calculated as the ratio of the mean area under the curve for one burst in a given time point data file, to the mean area under one burst at baseline as shown in the formula below:

$$SF = (\text{area TP}/\text{count TP})/(\text{area BL}/\text{count BL}),$$

where SF is scaling factor, area is area under each burst, count is burst count in the analyzed segment, TP is time point of experiment, and BL is baseline. Next, time point activity was multiplied by the scaling factor. RSNA is reported as arbitrary units.

2.5. Waveform analysis

EKG and arterial blood pressure waveforms were continuously monitored throughout the experiment and recorded at 500 Hz using an in-house digital data acquisition system during 15-min-long observation periods that followed each intervention (i.e. episodes of blood withdrawal, resuscitation or blood re-infusion). This allowed us to do the analysis on the most stable discrete data sets. Thus 7 time points (baseline, after bleed 1, after bleed 2, after bleed 3, after bleed 4, after LR resuscitation and after blood re-infusion) were analyzed for every subject. Next, off-line, 800-beat data sections from within each observation period were imported into the WinCPRS software. Automatic identification of R-waves was carried out by means of an iso-electric line-shift algorithm. We verified correct identification of each R-wave in every data set. The analyzed RRI data was free of ectopy. The software generated the instantaneous RRI and SAP time series. Before spectral calculations, signals were windowed with Hanning function and re-sampled with a 5 samples/second rate. The re-sampled signals were zero-padded to the next power of 2 before the FFT routine was used to calculate the power spectra. Next, the low-frequency (LF) power (frequency range: 0.04–0.15 Hz), and high-frequency (HF) power (frequency range: 0.15–0.4 Hz), components of the RRI were calculated for each data set with baseline normalization. Because of the large inter-animal variability in absolute values of the spectral data we normalized the spectral data to the total power (Anonymous, 1996). All data reported in this study are normalized spectral data. Normalization was achieved by dividing the integrated LF and HF spectra by the total power (minus oscillations occurring below 0.05 Hz) and multiplying this value by 100. The normalized, integrated areas within the LF band were divided by normalized areas in the HF band to derive the normalized ratio (LFnu/HFnu). This ratio was taken as an index of sympatho-vagal balance (Pagani et al., 1986).

For non-linear analysis, approximate entropy (ApEn), sample entropy (SampEn) and fractal dimension by curve lengths (FDCL) were calculated for the same 800-beat segments using the software. Eight hundred beats were selected as an optimal data size for analysis in order to prevent any bias in ApEn which is prone to changes in the number of data points (Pincus, 1995). Before entropy calculations, linear trends were removed in all segments of the analyzed data. For both ApEn and SampEn calculations the dimension parameter m was 2 and the filter parameter r was 20% of the standard deviation. Analysis algorithms are identical to those used by Kuusela et al. (2002).

2.6. Catecholamine assays

At each time point, 5 ml of arterial blood was collected into vacutainer tubes containing EDTA, and was centrifuged at 1000 g for 10 min. The obtained plasma was stored in polypropylene tubes at −80 °C until the day of the assay. Plasma samples were then thawed in the refrigerator and assayed according to He et al. (1997) with modifications. Epinine (25 μl of a 100 ng/ml solution) was added to each 1 ml plasma sample and served as the internal standard. Next, 1 ml of TRIS buffer (pH 9) and 50 mg of acid-washed alumina was added, followed by shaking for 15 min. Then, the samples were centrifuged at 1000 g for 5 min to precipitate the alumina, which was washed twice with 1 ml of TRIS buffer. The alumina was mixed with 150 μl of 0.1 M perchloric acid solution and vortexed for 1 min, than the

Table 1
Hemodynamic and catecholamine data

Time point	0	1	2	3	4	5	6	p^1	p^2	p^3
Event	Baseline	10 ml/kg	20 ml/kg	30 ml/kg	40 ml/kg	LR	Re-infusion	(0 vs. 2)	(0 vs. 4)	(2 vs. 4)
N	8	8	8	8	5	4	2			
HR	86±5	82±3	85±2	117±12	138±12	114±11	109±17	NS	<.0001	<.0001
SAP	101±6	74±5	48±5	38±3	29±3	99±18	109±34	<.0001	<.0001	<.0001
DAP	85±8	59±6	32±5	19±3	14±2	59±13	72±28	<.0001	<.0001	<.0001
CO	2.7±0.1	1.8±0.1	1.2±0.1	0.8±0.1	0.5±0.1	7.6±2.2	6.8±0.7	<.0001	<.0001	<.0001
Lactate	1.5±0.3	1.6±0.3	3.0±0.5	7.5±1.1	11.1±0.8	15.6±1.1	14.4±1.3	.041	<.001	<.001
Dop	74±37	85±47	53±12	118±23	265±77	164±31	119±53	NS	.008	.003
Epi	64±36	45±8	118±23	3652±137	14595±6149	611±222	262±106	NS	.002	.002
Norepi	382±97	429±88	501±63	1383±290	6901±3052	1095±210	1298±374	NS	.009	.011

Time point: baseline (0), after withdrawal of 10 (1), 20 (2), 30 (3) and 40 ml/kg (4) of blood; after resuscitation with lactated Ringer's (5); after re-infusion of shed blood (6). p^1, significance level when baseline compared with time point 2; p^2, significance level when baseline compared with time point 4; p^3, significance level when time point 2 compared with time point 4. *N*, sample size at each time point; HR, heart rate; SAP, systolic arterial pressure, mm Hg; DAP, diastolic arterial pressure, mm Hg; CO, cardiac output, l/min; lactate, plasma lactate levels in mmol/l; Dop, plasma dopamine, ng/ml; Epi, plasma epinephrine, ng/ml; Norepi, plasma norepinephrine, ng/ml. Data are means±SEM.

sample was centrifuged at 1000 *g* for 5 min. The supernatant was placed in microfilterfuge tubes and centrifuged for 2 min, and 100 μl of the sample was injected into the HPLC. For calculation of norepinephrine, epinephrine, and dopamine levels in plasma samples, ratios of peak areas of each catecholamine to the peak area of epinine were compared against those of a series of calibrators. The concentrations of the catecholamines were expressed in ng/ml. The HPLC system consisted of a Waters 515 pump, Waters 717 autosampler, Coulochem 2 electrochemical detector equipped with a 5011 detector cell, and an Alltima C18 column (5 μm, 4.6 (ID)×150 (length) mm). The mobile phase was 75 mM phosphate, 1.7 mM octanesulfonic acid, 25 μM EDTA, and 5% (v/v) acetonitrile in Milli-Q water. The flow rate of the mobile phase was 1.5 ml/min.

2.7. Statistics

Data analyses were carried out using SAS, version 8.1 (SAS Institute Inc. 1999). Variables measured at different times were analyzed using a mixed model ANOVA allowing for time as a fixed effect and replicate subject as a random effect. The covariance structure for the mixed model was determined using the Bayesian Information Criterion. Hochberg's step-up Bonferroni method was used for *p* value adjustment for multiple comparisons among time points. Log transformation was used when appropriate. Statistical significance was determined as $p<.05$.

3. Results

Hemorrhage resulted in severe shock, such that only 25% of animals survived until the end of the experiment. All animals survived removal of 30 ml/kg of blood at time point 3. Three animals died after bleed 3; one animal died after bleed 4; and two animals died after LR resuscitation. The physiologic data are summarized in Table 1. Heart rate did not change between baseline (86±5 bpm) and after bleeds 1 (82±30) or 2 (85±2), but peaked at 138±12 after bleed 4 ($p<.0001$). SAP decreased from 101±6 mm Hg to 48±5 after bleed 2 ($p<.0001$) and reached its nadir after bleed 4 at 29±3 mm Hg ($p<.0001$). Diastolic arterial pressure decreased progressively. Cardiac output decreased from 2.7±0.1 l/min at baseline, to 0.5 l/min after bleed 4

Table 2
Renal sympathetic nerve activity, linear and non-linear analysis data

Time point	0	1	2	3	4	5	6	p^1	p^2	p^3
Event	Baseline	10 ml/kg	20 ml/kg	30 ml/kg	40 ml/kg	LR	Re-infusion	(0 vs. 2)	(0 vs. 4)	(2 vs. 4)
N	8	8	8	8	5	4	2			
RSNA	586±61	848±163	1060±201	1014±312	216±91	1866±787	1435±1305	NS	.006	.001
LFnu	0.59±0.08	0.80±0.05	0.88±0.04	0.80±0.10	0.87±0.06	0.40±0.06	0.57±0.13	.009	.001	NS
HFnu	0.35±0.07	0.17±0.03	0.11±0.03	0.16±0.07	0.12±0.05	0.52±0.06	0.36±0.08	.003	.004	NS
LFnu/HFnu	3.25±1.37	6.57±1.74	11.99±2.42	9.31±1.72	20.07±8.50	0.83±0.17	1.75±0.77	.006	.007	NS
ApEn	0.91±0.11	0.84±0.13	0.82±0.14	0.62±0.11	0.59±0.09	0.90±0.16	0.99±0.03	NS	.033	NS
SampEn	0.90±0.14	0.85±0.17	0.79±0.15	0.57±0.11	0.52±0.09	0.83±0.22	0.96±0.04	NS	NS	NS
FDCL	1.72±0.04	1.70±0.03	1.65±0.03	1.50±0.05	1.49±0.06	1.53±0.02	1.75±0.06	NS	<.001	.003

Time point: baseline (0), after withdrawal of 10 (1), 20 (2), 30 (3) and 40 ml/kg (4) of blood; after resuscitation with lactated Ringer's (5); after re-infusion of shed blood (6). p^1, significance level when baseline compared with time point 2; p^2, significance level when baseline compared with time point 4; p^3, significance level when time point 2 compared with time point 4. *N*, sample size at each time point; RSNA, renal sympathetic nerve activity; LFnu, normalized low-frequency power of the RRI; HFnu, normalized high-frequency power of the RRI; LFnu/HFnu, ratio of the normalized low-frequency power to normalized high-frequency power of the RRI; ApEn, approximate entropy; SampEn, sample entropy; FDCL, RRI fractal dimension by curve lengths. Data are means±SEM.

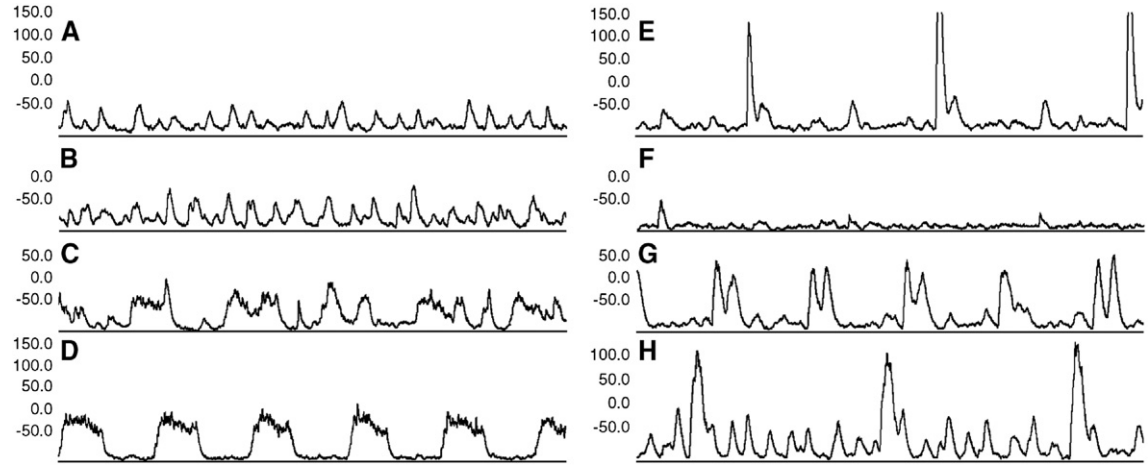

Fig. 1. Example of RSNA activity over time: A. baseline; B. during first bleed (500 ml of blood removed). Note a somewhat increased burst amplitude and area when compared to A; C. after 2nd bleed (980 ml of blood removed). Area under each burst increases further. Hyperpolarization and repetitive firings are evident; D. during the 3rd bleed (1150 ml of blood removed). Formation of hyperpolarized burst conglomerates; E. after the 4th and final bleed (1304 ml of blood removed). RSNA significantly decreased; F. 6 min after completion of 4th bleed. Sympathetic withdrawal; G. during resuscitation (1900 ml LR have been infused). Partial return of RSNA; H. after completion of resuscitation with LR, 3450 ml infused). Return of tonic RSNA.

($p<.0001$). Lactate increased significantly from 1.5±0.3 at baseline, to 11.1±0.8 mmol/l after bleed 4 ($p<.001$). Changes in base excess were similar (data not shown).

Plasma catecholamines increased significantly after bleed 4 (Table 1).

3.1. RSNA morphology

RSNA increased in 7/8 animals during HS, although the time point at which the highest value was reached varied among animals. Thus, it increased numerically but not significantly from a baseline value of 586±61 to a peak value of 1060±201 after withdrawal of 20 ml/kg of blood (Table 2). RSNA then decreased in all animals, reaching a nadir of 216±91 after bleed 4 when compared to both post bleed 2 ($p=.006$), and to the baseline ($p=.001$) (Table 2).

Fig. 1 shows the morphology of RSNA at each time point in one of the survivors of the full protocol. The pattern of multiple burst complexes depicted in Fig. 3D is one of the most pronounced of all seen in the study and was present in the two animals that survived the entire study. Similar changes—featuring grouping of consecutive bursts into doublets (Fig. 3B), triplets, and multiple bursts (Fig. 3C)—were observed as a function of progressive volume depletion in all animals. In the 4 animals surviving past the LR resuscitation, activity increased to more than 3 times the baseline value (1866±787) and at the end of the study, in the eventual 2 full survivors of the protocol the RSNA remained almost 300% of the baseline value.

3.2. Spectral analysis of EKG

RRI LFnu increased significantly from a baseline value of 0.59±0.08 to 0.88±0.04 after bleed 2 ($p=.009$) and was

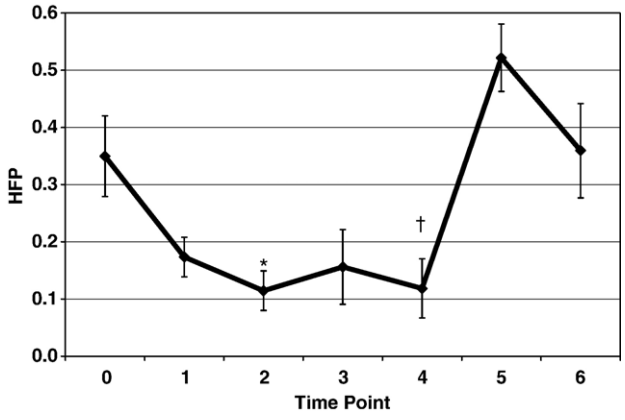

Fig. 2. Changes in the normalized RRI high-frequency power. *, $p=.003$, baseline vs. post bleed 2. †, $p=.004$, baseline vs. post bleed 4. See text for details.

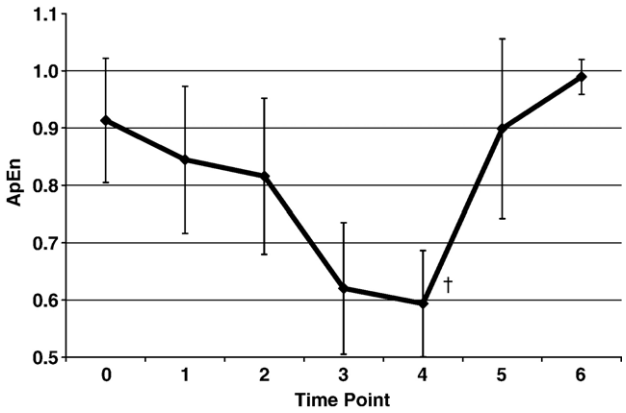

Fig. 3. Changes in approximate entropy. †, $p<.033$, baseline vs. post bleed 4. See text for details.

sustained at a higher level after bleed 4 when compared to baseline (Table 2). RRI HFnu decreased from baseline values (0.35±0.07) to a nadir (0.11±0.03) after bleed 2 (p=.003, Table 2, Fig. 2). After bleed 4, HFnu remained low compared to baseline (0.35±0.07 at baseline vs. 0.11±0.03 after bleed 2, p=.004) but was not different from the nadir point after bleed 2 (0.12±0.05, NS) (Fig. 2). The LFnu/HFnu ratio increased significantly after bleed 2 (p=.006) and remained elevated throughout the HS period and significantly higher than baseline after bleed 4 (p=.007) (Table 2). With the LFnu/HFnu remaining elevated, and RSNA showing withdrawal after bleed 4, a significant relationship between the LFnu/HFnu ratio and RSNA using all data points was not revealed by linear regression (p=.121, r^2=0.048, n=51).

3.3. Non-linear analysis of EKG

Both RRI ApEn and SampEn (Table 2) followed similar trends in this study, decreasing numerically after each blood withdrawal and reaching the lowest values after bleed 4 at which point changes in ApEn were significant (ApEn: 0.91±0.11 at baseline vs. 0.59±0.09, p=.033, Table 2, Fig. 3). The fractal dimension by curve lengths (FDCL) progressively decreased with each blood withdrawal from a baseline of 1.72±0.04 to a nadir of 1.49±0.06 following bleed 4 (p<.001). This FDCL value after bleed 4 was also significantly lower when compared to post bleed 2 (p=.003) (Table 2).

4. Discussion

We examined changes in RSNA in response to a highly lethal model of hemorrhagic shock (HS) in anesthetized sheep, and assessed the relationship between non-invasive indexes of cardiac autonomic regulation and RSNA. There were 4 principal findings: (1) moderate blood loss of 20 ml/kg caused hypotension, morphologic evidence of RSNA activation, and increases in LFnu, LFnu/HFnu ratio and plasma catecholamine levels; (2) severe blood loss of 40 ml/kg led to RSNA withdrawal, sustained LFnu and LFnu/HFnu ratio, and continued increases in catecholamine levels; (3) all stages of blood withdrawal were associated with a decrease in the RRI HFnu; and (4) blood withdrawal led to decreases in RRI complexity, measured by ApEn and FDCL.

RSNA morphology changed as a function of volume status. Despite some degree of inter-animal variability in RSNA response to hemorrhage, 7 out of 8 animals demonstrated increasing burst frequency with volume depletion. The amplitude and area under each burst also increased and grouping of bursts into doublets and triplets took place as more blood was withdrawn. Eventually, burst conglomerates formed before the onset of sympathetic withdrawal in survivors. To our knowledge, this is the first report on RSNA burst conglomerate formation during severe hemorrhagic shock. Conglomeration of bursts may indicate the accumulation of multiple action potential firings (Tang et al., 2003), possibly providing for a stronger sympathetic discharge in the face of progressive volume loss. With repetitive and superimposed firings hyperpolarization may then take place, which may lead to neuronal hyperexcitability (Kandel et al., 1991) and the development of multiple burst complexes (Fig. 3C–D). Development of these complexes may be a "last resort" compensatory mechanism during pre-terminal shock, and may be caused by altered neuronal recruitment, altered firing patterns, and/or prolonged neurotransmitter release eventually leading to receptor saturation. Such multiple burst complexes, seen in the two full survivors, may characterize subjects with adequate autonomic reserves to withstand near-lethal hypotension.

Sympathetic withdrawal occurred in all surviving subjects after blood loss of 40 ml/kg. Skoog et al. (1985) found short-lasting sympathetic activation followed by powerful sympathetic inhibition as assessed by RSNA measurements in anesthetized hemorrhaged rats. The authors proposed that the observed sympathetic inhibition was mediated by mechanically sensitive cardiac vagal afferents triggered by markedly decreased cardiac filling (Skoog et al., 1985). Koyama et al. (1988) reported decreased sympathetic activity in their studies on anesthetized dogs subjected to hemorrhage, and proposed that prolonged brain ischemia causes depression of sympathetic outflow in shock. Sympathetic withdrawal was suggested to represent a fundamental mechanism for the development of circulatory shock in humans subjected to lower-body negative pressure (Convertino et al., 2004). Our findings support observations in the literature that severe hemorrhage may cause a failure of compensation characterized by a decrease in sympathetic nerve activity.

A decrease in RRI HFnu occurred during HS, consistent with withdrawal of vagal modulation to the heart (Palazzolo et al., 1998). Previously, we identified a decrease in RRI HF in anesthetized swine subjected to isovolemic hemorrhagic shock (Batchinsky et al., 2007). Similarly, Palazzolo et al. (1998) documented loss of vagally mediated RRI oscillations during hypotension in conscious dogs.

RSNA and LFnu/HFnu ratio did not correlate in our study. This dissociation between direct microneurographic measurements of sympathetic tone and indirect non-invasive estimates of autonomic modulation derived from heart rate variability analysis has been reported in other settings as well. For example, Pagani et al. found a good correlation between LFnu of HRV and LFnu of muscle sympathetic nerve activity (MSNA) variability, but not between LFnu (or LFnu/HFnu) of HRV and MSNA burst rate in humans (Pagani et al., 1997). Floras et al. (2001) did not find within-subject correlations between MSNA and LF/HF ratio during lower-body negative pressure (Floras et al., 2001). Cooke and Dowlyn (2000) found that RRI spectral analysis did not adequately reveal subtle changes in sympathetic traffic during head-down tilt as assessed by muscle sympathetic nerve activity. As shown by Kingwell et al. (1994) in patients with heart failure, cardiac sympathetic nerve firing measured with standard spillover techniques and LF changed in opposite directions. Thus, the dissociation between direct tonic and indirect HRV measures of autonomic activity is a predominant finding in the literature. Additionally, the concept of differential

activation of the autonomic nervous system in various vascular beds may be an additional reason for the discrepancy between the indirect measures of autonomic modulation of the heart (HRV) and direct measures of sympathetic tone (Ninomiya et al., 1971; Barman et al., 1984). For example, Barman et al. (1984) demonstrated that in cats the reticular formation controls the sympathetic discharge to cardiac, renal and carotid nerves in a non-uniform fashion. Direct cardiac sympathetic nerve activity measurements (Jardine et al., 2005) will likely provide more decisive evidence on the relationship between indirect HRV metrics and tonic sympathetic traffic in the heart. Meanwhile, however, our findings support the evidence in the literature that changes in surrogate measures of cardiac autonomic modulation such as LFnu/HFnu ratio, do not correlate with direct measures of tonic sympathetic discharge in the renal vascular bed.

In recent years, non-linear statistical methods have increasingly been applied to the analysis of the EKG. These methods are designed to analyze dynamically changing non-stationary data (Anonymous, 1996) such as those explored in this study. Complexity is a fundamental characteristic of normal physiologic time series, such as the RRI. It has been suggested that loss of complexity or "decomplexification" is a feature of disease (Goldberger and West, 1987) and of impaired adaptation to stress (Lipsitz and Goldberger, 1992). Complexity can be assessed by methods such as approximate entropy (ApEn). ApEn quantifies the probability of encountering a similar pattern within the signal at the next incremental comparison (Pincus, 1995); it is affected by the number of data points. SampEn is a similar approach, in which the vector comparison with itself is removed; this makes this method independent, in theory, of the number of data points (Richman and Moorman, 2000). Entropy is high in irregular, complex signals and decreases as the signals become more regular. In our study, both entropy metrics (ApEn and SampEn) showed similar trends decreasing numerically with each blood withdrawal and reached a nadir after the 4th bleed at which point the values for ApEn were significantly lower when compared to baseline (changes in SampEn were non-significant). These findings are consistent with our previous work that identified a decrease in ApEn and SampEn during isovolemic hemorrhagic shock in anesthetized swine (Batchinsky et al., 2007). Palazzolo et al. (1998) identified a decrease in ApEn during hypotension in conscious dogs. Complexity in our current study changed in opposite direction to the indirect measures of autonomic cardiac modulation, LFnu and LFnu/HFnu. This is in agreement with Porta et al. who used a new entropy calculation approach, the corrected conditional entropy method, and found loss of complexity in the presence of increased LFnu during head-up tilt in humans (Porta et al., 2000) and during nitroprusside infusion or handgrip (Porta et al., 2007). Corrected conditional entropy is a promising tool which allows for analysis of shorter data sequences without a-priori selection of the embedding dimension (Porta et al., 1998), unlike ApEn and SampEn. Further studies will be needed to define the optimal entropy method.

Another measure of complexity, FDCL, is a fractal image analysis method that describes changes in the structure of the RRI time series by evaluating the number of short segments or "sticks" necessary to follow the signal curve (Chau et al., 1993, Kuusela et al., 2002). A higher FDCL value indicates an exponential increase in the number of sticks required to describe the structure of the signal, implying higher complexity. The decrease in fractal dimension metrics identified in this study has been previously documented by us during isovolemic hemorrhagic shock in swine (Batchinsky et al., 2007). These data are also consistent with the findings by West et al., who reported a decrease in the fractal dimension of the RRI during lower-body negative pressure in humans (West et al., 2004).

At this point, loss of complexity during HS maybe related to decreased vagal activity, since it correlated with decreased HFnu in both this and other studies (Palazzolo et al., 1998; Kuusela et al., 2002; Batchinsky et al., 2007). Alternatively, loss of complexity may also be viewed as a non-specific marker of physiologic deterioration under conditions of hypovolemia or critical illness.

5. Conclusions

In an anesthetized ovine model of highly lethal hemorrhagic shock, moderate hypotension (blood loss of 20 ml/kg) was associated with an increase in the RRI LF/HF ratio (an indirect frequency-domain index of sympatho-vagal balance), and a decrease in the RRI HF (an index of vagal activity). Directly measured tonic RSNA featured increases in the burst frequency, amplitude, and area; coupling of bursts into doublets and triplets; and, finally, formation of burst conglomerates. Blood loss of 40 ml/kg led to RSNA withdrawal. LF/HF did not correlate linearly with RSNA. RRI complexity, measured by ApEn and fractal dimension methods, decreased after completion of the 40 ml/kg hemorrhage. Measures of RRI complexity may provide useful information about patient status during hypovolemia. Further work will be needed, however, to understand the relationship between directly measured autonomic nerve activity and various indirect measures of autonomic modulation of the heart.

Acknowledgments

We are grateful to Dr. Marty Javors at the University of Texas Health Science Center at San Antonio for the analysis of the plasma samples for catecholamine levels. We are also grateful to Dr. Charles Wade for helpful comments on the manuscript.

The study was funded by the Combat Casualty Care Research Program of the US Army Medical Research and Materiel Command, Ft. Detrick, Maryland.

References

Akselrod, S., Gordon, D., Ubel, F.A., Shannon, D.C., Berger, A.C., Cohen, R.J., 1981. Power spectrum analysis of heart rate fluctuation: a quantitative probe of beat-to-beat cardiovascular control. Science 213, 220–222.

Anonymous, 1996. Heart rate variability: standards of measurement, physiological interpretation and clinical use. Task Force of the European Society of Cardiology and the North American Society of Pacing and Electrophysiology. Circulation 93, 1043–1065.

Barman, S.M., Gebber, G.L., Calaresu, F.R., 1984. Differential control of sympathetic nerve discharge by the brain stem. Am. J. Physiol. 247, R513–R519.

Batchinsky, A.I., Cooke, W.H., Kuusela, T., Cancio, L.C., 2007. Loss of complexity characterizes the heart-rate response to experimental hemorrhagic shock in swine. Crit. Care Med. 35, 519–525.

Butler, G.C., Yamamoto, Y., Hughson, R.L., 1994. Fractal nature of short-term systolic BP and HR variability during lower body negative pressure. Am. J. Physiol. 267, R26–R33.

Chau, N.P., Chanudet, X., Bauduceau, B., Gautier, D., Larroque, P., 1993. Fractal dimension of heart rate and blood pressure in healthy subjects and in diabetic subjects. Blood Press 2, 101–107.

Convertino, V.A., Ludwig, D.A., Cooke, W.H., 2004. Stroke volume and sympathetic responses to lower-body negative pressure reveal new insight into circulatory shock in humans. Auton. Neurosci. 111, 127–134.

Cooke, W.H., Dowlyn, M.M., 2000. Power spectral analysis imperfectly informs changes in sympathetic traffic during acute simulated microgravity. Aviat. Space Environ. Med. 71, 1232–1238.

Cooke, W.H., Hoag, J.B., Crossman, A.A., Kuusela, T.A., Tahvanainen, K.U., Eckberg, D.L., 1999. Human responses to upright tilt: a window on central autonomic integration. J. Physiol. 517 (Pt 2), 617–628.

Cooke, W.H., Salinas, J., Convertino, V.A., Ludwig, D.A., Hinds, D., Duke, J.H., Moore, F.A., Holcomb, J.B., 2006. Heart rate variability and its association with mortality in prehospital trauma patients. J. Trauma 60, 363–370.

Eckberg, D.L., 1997. Sympathovagal balance: a critical appraisal. Circulation 96, 3224–3232.

Evans, R.G., Ventura, S., Dampney, R.A., Ludbrook, J., 2001. Neural mechanisms in the cardiovascular responses to acute central hypovolaemia. Clin. Exp. Pharmacol. Physiol. 28, 479–487.

Floras, J.S., Butler, G.C., Ando, S.I., Brooks, S.C., Pollard, M.J., Picton, P., 2001. Differential sympathetic nerve and heart rate spectral effects of nonhypotensive lower body negative pressure. Am. J. Physiol., Regul. Integr. Comp. Physiol. 281, R468–R475.

Goldberger, A.L., West, B.J., 1987. Fractals in physiology and medicine. Yale J. Biol. Med. 60, 421–435.

Goldstein, B., Mickelsen, D., Want, A., Tipton, R., Cox, C., Woolf, P.D., 1999. Effect of *N*(G)-nitro-L-arginine methyl ester on autonomic modulation of heart rate variability during hypovolemic shock. Crit. Care Med. 27, 2239–2245.

Grossman, P., Wilhelm, F.H., Spoerle, M., 2004. Respiratory sinus arrhythmia, cardiac vagal control, and daily activity. Am. J. Physiol, Heart Circ. Physiol. 287, H728–H734.

He, H., Stein, C.M., Christman, B., Wood, A.J., 1997. Determination of catecholamines in sheep plasma by high-performance liquid chromatography with electrochemical detection: comparison of deoxyepinephrine and 3,4-dihydroxybenzylamine as internal standard. J. Chromatogr., B, Biomed. Sci. Appl. 701, 115–119.

Jardine, D.L., Charles, C.J., Ashton, R.K., Bennett, S.I., Whitehead, M., Frampton, C.M., Nicholls, M.G., 2005. Increased cardiac sympathetic nerve activity following acute myocardial infarction in a sheep model. J. Physiol. 565, 325–333.

Kandel, E.R., Schwartz, J.H., Jessell, T.M., 1991. Principles of Neural Science. Appleton and Lange, East Norwalk, CT.

Kawase, M., Komatsu, T., Nishiwaki, K., Kimura, T., Fujiwara, Y., Takahashi, T., Shimada, Y., 2000. Heart rate variability during massive hemorrhage and progressive hemorrhagic shock in dogs. Can. J. Anaesth. 47, 807–814.

Kingwell, B.A., Thompson, J.M., Kaye, D.M., McPherson, G.A., Jennings, G.L., Esler, M.D., 1994. Heart rate spectral analysis, cardiac norepinephrine spillover, and muscle sympathetic nerve activity during human sympathetic nervous activation and failure. Circulation 90, 234–240.

Koyama, S., Aibiki, M., Kanai, K., Fujita, T., Miyakawa, K., 1988. Role of central nervous system in renal nerve activity during prolonged hemorrhagic shock in dogs. Am. J. Physiol. 254, R761–R769.

Koyama, S., Sawano, F., Matsuda, Y., Saeki, Y., Shibamoto, T., Hayashi Jr., T., Matsubayashi, Y., Kawamoto, M., 1992. Spatial and temporal differing control of sympathetic activities during hemorrhage. Am. J. Physiol. 262, R579–R585.

Kuusela, T.A., Jartti, T.T., Tahvanainen, K.U., Kaila, T.J., 2002. Nonlinear methods of biosignal analysis in assessing terbutaline-induced heart rate and blood pressure changes. Am. J. Physiol, Heart Circ. Physiol. 282, H773–H783.

Lipsitz, L.A., Goldberger, A.L., 1992. Loss of 'complexity' and aging. Potential applications of fractals and chaos theory to senescence. JAMA 267, 1806–1809.

Madwed, J.B., Cohen, R.J., 1991. Heart rate response to hemorrhage-induced 0.05-Hz oscillations in arterial pressure in conscious dogs. Am. J. Physiol. 260, H1248–H1253.

Malpas, S.C., Evans, R.G., Head, G.A., Lukoshkova, E.V., 1998. Contribution of renal nerves to renal blood flow variability during hemorrhage. Am. J. Physiol. 274, R1283–R1294.

Ninomiya, I., Nisimaru, N., Irisawa, H., 1971. Sympathetic nerve activity to the spleen, kidney, and heart in response to baroceptor input. Am. J. Physiol. 221, 1346–1351.

Notarius, C.F., Floras, J.S., 2001. Limitations of the use of spectral analysis of heart rate variability for the estimation of cardiac sympathetic activity in heart failure. Europace 3, 29–38.

Pagani, M., Lombardi, F., Guzzetti, S., Rimoldi, O., Furlan, R., Pizzinelli, P., Sandrone, G., Malfatto, G., Dell'Orto, S., Piccaluga, E., et al., 1986. Power spectral analysis of heart rate and arterial pressure variabilities as a marker of sympatho-vagal interaction in man and conscious dog. Circ. Res. 59, 178–193.

Pagani, M., Montano, N., Porta, A., Malliani, A., Abboud, F.M., Birkett, C., Somers, V.K., 1997. Relationship between spectral components of cardiovascular variabilities and direct measures of muscle sympathetic nerve activity in humans. Circulation 95, 1441–1448.

Palazzolo, J.A., Estafanous, F.G., Murray, P.A., 1998. Entropy measures of heart rate variation in conscious dogs. Am. J. Physiol. 274, H1099–H1105.

Parati, G., Saul, J.P., Di Rienzo, M., Mancia, G., 1995. Spectral analysis of blood pressure and heart rate variability in evaluating cardiovascular regulation. A critical appraisal. Hypertension 25, 1276–1286.

Parati, G., Mancia, G., Di Rienzo, M., Castiglioni, P., 2006. Point: cardiovascular variability is/is not an index of autonomic control of circulation. J. Appl. Physiol. 101, 676–678 (discussion 681-672).

Pincus, S., 1995. Approximate entropy (ApEn) as a complexity measure. Chaos 5, 110–117.

Porta, A., Baselli, G., Liberati, D., Montano, N., Cogliati, C., Gnecchi-Ruscone, T., Malliani, A., Cerutti, S., 1998. Measuring regularity by means of a corrected conditional entropy in sympathetic outflow. Biol. Cybern. 78, 71–78.

Porta, A., Guzzetti, S., Montano, N., Pagani, M., Somers, V., Malliani, A., Baselli, G., Cerutti, S., 2000. Information domain analysis of cardiovascular variability signals: evaluation of regularity, synchronisation and co-ordination. Med. Biol. Eng. Comput. 38, 180–188.

Porta, A., Guzzetti, S., Furlan, R., Gnecchi-Ruscone, T., Montano, N., Malliani, A., 2007. Complexity and nonlinearity in short-term heart period variability: comparison of methods based on local nonlinear prediction. IEEE Trans. Biomed. Eng. 54, 94–106.

Richman, J.S., Moorman, J.R., 2000. Physiological time-series analysis using approximate entropy and sample entropy. Am. J. Physiol, Heart. Circ. Physiol. 278, H2039–H2049.

Saul, J.P., Rea, R.F., Eckberg, D.L., Berger, R.D., Cohen, R.J., 1990. Heart rate and muscle sympathetic nerve variability during reflex changes of autonomic activity. Am. J. Physiol. 258, H713–H721.

Secher, N.H., Jacobsen, J., Friedman, D.B., Matzen, S., 1992. Bradycardia during reversible hypovolaemic shock: associated neural reflex mechanisms and clinical implications. Clin. Exp. Pharmacol. Physiol. 19, 733–743.

Skoog, P., Mansson, J., Thoren, P., 1985. Changes in renal sympathetic outflow during hypotensive haemorrhage in rats. Acta Physiol. Scand. 125, 655–660.

Tang, X., Chander, A.R., Schramm, L.P., 2003. Sympathetic activity and the underlying action potentials in sympathetic nerves: a simulation. Am. J. Physiol., Regul. Integr. Comp. Physiol. 285, R1504–R1513.

West, B.J., Scafetta, N., Cooke, W.H., Balocchi, R., 2004. Influence of progressive central hypovolemia on Holder exponent distributions of cardiac interbeat intervals. Ann. Biomed. Eng. 32, 1077–1087.

Winchell, R.J., Hoyt, D.B., 1996. Spectral analysis of heart rate variability in the ICU: a measure of autonomic function. J. Surg. Res. 63, 11–16.